Contribution from the Department of Chemistry, North Carolina State University, Raleigh, North Carolina 27695-8204, and Departament de Quimica Inorgànica, Universitat de Barcelona, 08028 Barcelona, Spain

Importance of the X_4 Ring Orbitals for the Semiconducting, Metallic, or Superconducting Properties of Skutterudites MX_3 and RM_4X_{12}

Dongwoon Jung,[†] Myung-Hwan Whangbo,*,[†] and Santiago Alvarez*,[‡]

To gain insight into the electronic properties of binary and ternary skutterudite (i.e., $CoAs_3$-type) compounds, we performed tight-binding band electronic structure calculations on a prototype skutterudite $LaFe_4P_{12}$. The major contribution to the highest occupied band of $LaFe_4P_{12}$ comes from the orbitals of the P_4 rings that form the phosphorus sublattice. Consequently, the superconductivity of $LaFe_4P_{12}$ seems to be associated largely with the electrons of the phosphorus sublattice. Our calculations suggest that the t_{2g}- and e_g-block bands of all skutterudites should be separated by a band gap. Thus, skutterudites are expected to be semiconducting if their transition-metal electron count is d^6 but metallic in other cases.

The skutterudite (i.e., $CoAs_3$-type) structure is found for binary transition-metal compounds MX_3 (M = Co, Rh, Ir, X = P, As, Sb; M = Ni, Pd, X = P)[1-7] and also for ternary transition-metal compounds RM_4X_{12} (R = rare-earth metal, M = Fe, Ru, Os, X = P, As, Sb).[8-12] In all these skutterudite structures, each transition-metal atom is surrounded by six X_4 (nearly square) rings to form an octahedral coordination. Many skutterudite compounds are metals, and the ternary phosphides LaM_4P_{12} (M = Fe, Ru, Os) are superconductors with the superconducting transition temperatures T_c = 4.1, 7.2, and 1.8 K, respectively,[13] which are rather high for compounds of the iron group.[14] So far no band electronic structure calculations have been reported for this interesting class of compounds, although a two-electron bond model has been proposed[8,9] to explain their electrical properties. In the present work the electronic structure of a prototype skutterudite, i.e., $LaFe_4P_{12}$,[8] is calculated by employing the tight-binding method[15] within the extended Hückel[16] framework. We then examine how the calculated band electronic structure of $LaFe_4P_{12}$ is related to its crystal structure and discuss the electrical properties of other skutterudite compounds. The atomic parameters employed in our calculations are summarized in Table I.

Crystal Structure

In understanding the nature of the highest occupied (HO) band of $LaFe_4P_{12}$, which is partially filled and therefore responsible for its normal metallic properties, it is important to know its crystal structure. The phosphorus atoms of $LaFe_4P_{12}$ occur in the form of P_4 rings, which are nearly square (See **1**. For simplicity, each P_4 ring **1a** is represented by **1b**.). The arrangement of six P_4 rings

1a   **1b**
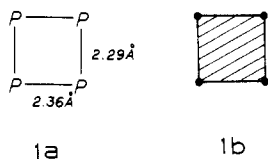
around an Fe atom can be conveniently described in terms of a cube, as depicted in **2**. The center of the cube contains an Fe


2
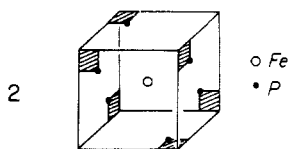
atom, and each face of the cube contains a quarter of one P_4 ring (shown by a shaded square, in which a filled circle represents a phosphorus atom), with the center of a P_4 ring located at each cube corner. Thus, the octahedral coordination of Fe is provided by six different P_4 rings. The body-centered unit cell of $LaFe_4P_{12}$

Table I. Atomic Parameters Used in the Tight-Binding Calculations: H_{ii} (eV) and ζ (Valence Orbital Ionization Potential and Exponent of the Slater Type Orbital)[a,b]

atom	orbital	H_{ii}	ζ_1 (c_1)	ζ_2 (c_2)
Fe	4s	−9.10	1.9	
	4p	−5.32	1.9	
	3d	−12.6	5.35 (0.5505)	2.0 (0.6260)
P	3s	−18.6	1.6	
	3p	−14.0	1.6	
Sb	5s	−18.8	2.323	
	5p		see Figure 5	

[a] The d orbital of Fe is given as a linear combination of two Slater type orbitals, and each exponent is followed by the weighting coefficient in parentheses. [b] A modified Wolfsberg-Helmholz formula was used to calculate H_{ij}.[28]

is constructed by assembling eight such cubes, as schematically shown in **3**, where thick line segments represent cross sections of


3
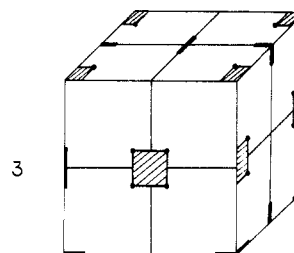
P_4 rings. Each phosphorus atom coordinates two different Fe atoms in neighboring cubes, which suggests that each phosphorus atoms has two nonbonding electron pairs; i.e., the formal oxidation

---

[†] North Carolina State University.
[‡] Universitat de Barcelona.

(1) Pearson, W. B. *A Handbook of Lattice Spacings and Structures of Metals and Alloys*; Pergamon Press: New York, 1967; Vol. 2.
(2) Rundqvist, S.; Ersson, N. O. *Ark. Kemi* **1968**, *30*, 103.
(3) Rundqvist, S.; Ersson, N. O. *Ark. Kemi* **1964**, *23*, 335.
(4) Kjekshus, A.; Pedersen, G. *Acta Crystallogr.* **1961**, *14*, 1065.
(5) Mandel, N.; Donohue, J. *Acta Crystallogr.* **1971**, *B27*, 2288.
(6) Kjekshus, A.; Rakke, T. *Acta Chem. Scand.* **1974**, *A28*, 99.
(7) Zhuravlev, N. N.; Zhdanov, G. S. *Sov. Phys.—Crystallogr. (Engl. Transl.)* **1956**, *1*, 404.
(8) Jeitschko, W.; Braun, D. J. *Acta Crystallogr.* **1977**, *B33*, 3401.
(9) Grandjean, F.; Gérard, A.; Braun, D. J.; Jeitschko, W. *J. Phys. Chem. Solids* **1984**, *45*, 877.
(10) Braun, D. J.; Jeitschko, W. *J. Solid State Chem.* **1980**, *32*, 357.
(11) Braun, D. J.; Jeitschko, W. *J. Less-Common Met.* **1980**, *72*, 147.
(12) Braun, D. J.; Jeitschko, W. *J. Less-Common Met.* **1980**, *76*, 33.
(13) Meisner, G. P. *Phys. B* **1981**, *108B*, 763.
(14) Cashion, J. D.; Shenoy, G. K.; Niarchos, D.; Viccaro, P. J.; Falco, C. M. In *Nuclear and Electron Resonance Spectroscopies Applied to Materials Sciences*; Kaufmann, E., Shenoy, G. K., Eds.; Elsevier North-Holland: New York, 1981; p 315.
(15) Whangbo, M.-H.; Hoffmann, R. *J. Am. Chem. Soc.* **1978**, *100*, 6093.
(16) Hoffmann, R. *J. Chem. Phys.* **1963**, 1397.

state of phosphorus is −1. It is important to observe from **3** that LaFe$_4$P$_{12}$ has linear arrays of P$_4$ rings in each crystallographic direction, as schematically shown in **4**, where adjacent P$_4$ rings
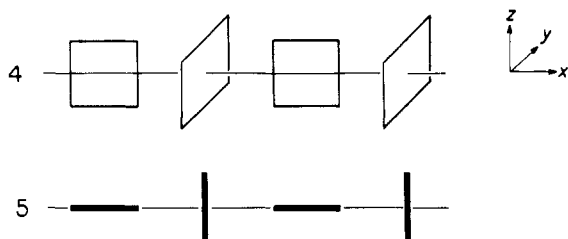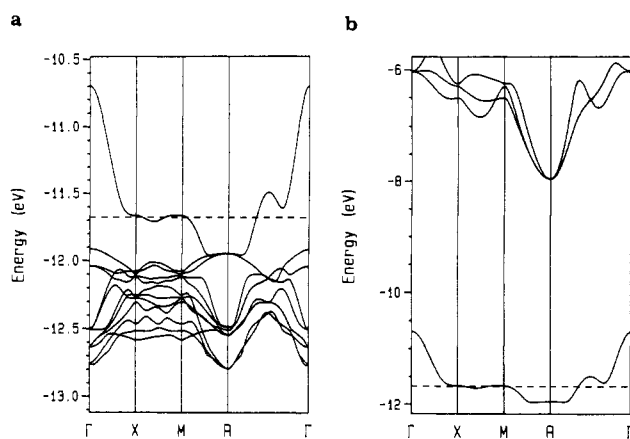
are orthogonal to each other. Thus, in each crystallographic direction, one phosphorus atom of a P$_4$ ring makes two short P···P contacts (2.97 Å) with the adjacent P$_4$ ring, which are substantially shorter than the van der Waals radii sum of two phosphorus atoms (i.e., 3.7 Å).[17] In fact, vibrational spectroscopic studies[18,19] on MX$_3$ skutterudites (X = P, As, Sb) show that the intraring P–P stretching frequencies are strongly coupled with the interring P···P stretching frequencies. For our discussion in the next section, it is convenient to represent an array of P$_4$ rings **4** in terms of its projection view **5**. In the unit cell **3**, La^{3+} cations are located at the six eight-coordinate sites provided by four adjacent P$_4$ rings, i.e., at the midpoints of the four horizontal edges and the centers of the two vertical faces of **3**. Thus, the unit cell of the body-centered cubic structure is given by 2(LaFe$_4$P$_{12}$).
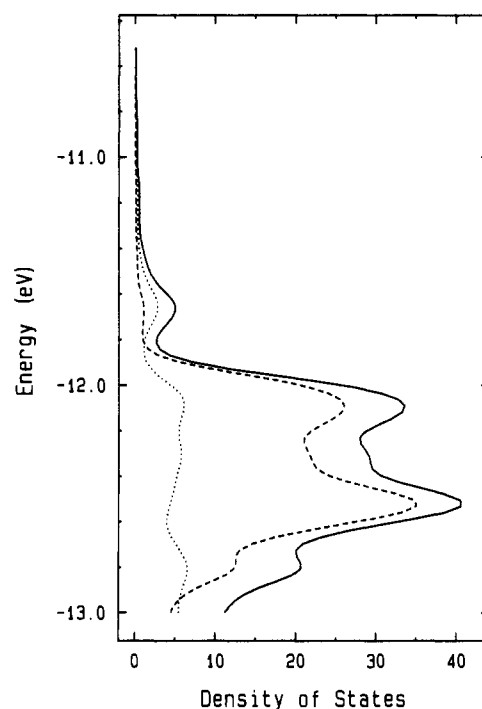
Electronic Structure

To reduce the computational task of our band calculations on LaFe$_4$P$_{12}$, we employ the primitive unit cell instead of the body-centered unit cell. The unit cell size of the former is half that of the latter. To further simplify our task, we omit La^{3+} cations from our calculations. Therefore, the primitive unit cell employed in our study has the formula Fe$_4$P$_{12}$$^{3-}$.

A. Band Electronic Structure. Part a of Figure 1 shows the dispersion relations of the t$_{2g}$-block bands calculated for the Fe$_4$P$_{12}$$^{3-}$ lattice, where the dashed line refers to the Fermi level. Given the formal oxidation states La^{3+} and P$^-$, the oxidation state of Fe becomes +2.25. For the unit cell Fe$_4$P$_{12}$$^{3-}$, there are 23 electrons to fill the 12 t$_{2g}$-block bands, so that the HO band is half-filled. Part b of Figure 1 shows that the bottom portion of the e$_g$-block bands is separated from the HO band by an indirect gap of about 2.7 eV.

It is noted from part a of Figure 1 that the HO band is most dispersive among the t$_{2g}$-block bands. Since this band is responsible for the metallic properties of LaFe$_4$P$_{12}$, we now examine its nature. The total and projected density of states (DOS) calculated for the t$_{2g}$-block bands are shown in Figure 2, where the solid line refers to the total DOS while the dashed and dotted lines represent the contributions of the Fe 3d and the phosphorus 3s/3p orbitals, respectively. Below −11.9 eV the total DOS is dominated by the Fe 3d orbitals but above −11.9 eV by the phosphorus orbitals. The Fermi level, e$_f$ (≈−11.7 eV) occurs in the energy region where the Fe 3d orbital character is negligible, so that the empty region of the HO band is due mainly to the phosphorus atoms. Simply speaking, therefore, the metal t$_{2g}$-block levels are nearly filled, while the phosphorus valence band top, which goes above the t$_{2g}$-block band of iron, becomes partially empty. In terms of this observation, the actual oxidation states of iron and phosphorus may be closer to Fe^{2+} and P$^{11/12-}$ rather than Fe$^{2.25+}$ and P$^-$, respectively. This picture is consistent with the conclusions of the Mössbauer studies that LaFe$_4$P$_{12}$ contains only one kind of iron atom with practically no magnetic moment.[9,20]

Figure 1. Dispersion relations of the d-block bands calculated for LaFe$_4$P$_{12}$: (a) the t$_{2g}$-block bands and (b) the highest occupied (HO) band of the t$_{2g}$-block and the e$_g$-block band bottom.

**Figure 2.** Total and projected DOS (electrons/eV) calculated for the t$_{2g}$-block bands of LaFe$_4$P$_{12}$, where the solid line refers to the total DOS. The contributions of the Fe 3d and the phosphorus orbitals to the total DOS are shown by the dashed and the dotted lines, respectively.

B. Nature of the HO Band. As discussed above, the HO band of LaFe$_4$P$_{12}$ has mainly phosphorus character. Since this band is largely responsible for the metallic properties of LaFe$_4$P$_{12}$, we examine its orbital nature. With the formal oxidation state of P$^-$, the P$_4$$^{4-}$ ring has eight occupied orbitals resulting from the two unshared electron pairs on each phosphorus. Figure 3 shows the upper four of these eight orbitals calculated for the P$_4$$^{4-}$ ring **1a**. In this ring, the "vertical" P–P bond is shorter than the "horizontal" P–P bond, so the π_3 orbital lies slightly higher in energy than the π_2 orbital. The π_4 orbital is the HOMO of the P$_4$$^{4-}$ ring, which is antibonding in each P–P bond. In the

(17) Bondi, A. *J. Phys. Chem.* **1964**, *68*, 441.
(18) Lutz, H. D.; Kliche, G. *Z. Anorg. Allg. Chem.* **1981**, *480*, 105.
(19) Lutz, H. D.; Kliche, G. *Phys. Status Solidi* **1982**, *B112*, 549.
(20) Shenoy, G. K.; Noakes, D. R.; Meisner, G. P. *J. Appl. Phys.* **1982**, *53*, 2628.
(21) DeLong, L. E.; Meisner, G. P. *Solid State Commun.* **1985**, *53*, 119.
(22) Odile, J. P.; Soled, S.; Castro, C. A.; Wold, A. *Inorg. Chem.* **1978**, *17*, 283.

(23) Pleass, C. M.; Heyding, R. D. *Can. J. Chem.* **1962**, *40*, 590.
(24) Dudkin, L. D.; Abrikosov, N. Kh. *Sov. Phys.—Solid State (Engl. Transl.)* **1959**, *1*, 126.
(25) Hulliger, F. *Helv. Phys. Acta* **1961**, *34*, 782.
(26) Ackerman, J.; Wold, A. *J. Phys. Chem. Solids* **1977**, *38*, 1013.
(27) Meisner, G. P.; Torikachvili, M. S.; Yang, K. N.; Maple, M. B.; Guertin, R. P. *J. Appl. Phys.* **1985**, *57*, 3073.
(28) Ammeter, J. H.; Bürgi, H.-B.; Thibeault, J. C.; Hoffmann, R. *J. Am. Chem. Soc.* **1978**, *100*, 3686.
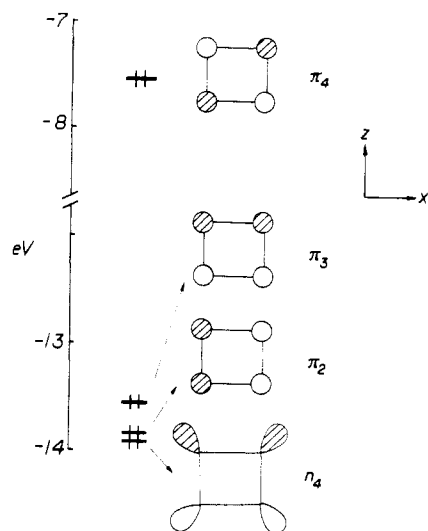
Figure 3. Highest four occupied molecular orbitals calculated for the P_4^{4-} ring of $LaFe_4P_{12}$.

framework of the projection view **5**, where each line represents a P_4^{4-} ring, the projection views of π_4, π_3 and n_4 on the xy plane (using the local coordinates of Figure 3) can be given by **6a**, **7a**, and **8a**, respectively. When the P_4^{4-} ring is rotated around the

6a   6b

7a   7b

8a   8b
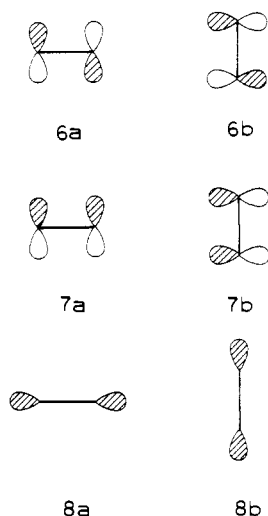
z axis by 90°, the corresponding projection views of π_4, π_3, and n_4 on the xy plane are given by **6b**, **7b**, and **8b**, respectively. Then the top of the HO band of $LaFe_4P_{12}$, which occurs at Γ, is given as the most antibonding combination of π_4 orbitals along each crystallographic direction, as depicted in **9**. All the short interring

9

π_4 π_4
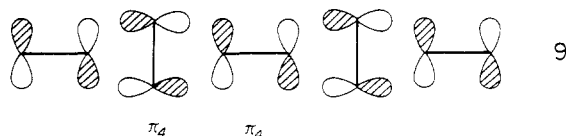
P···P contacts have antibonding interactions in **9**, thereby raising the resulting band energy at Γ. The phosphorus p orbitals at Γ generate a local symmetry A_{2u} (D_{3d} point group) around each Fe, so that they cannot combine with the Fe 3d orbitals but they can with the Fe 4p orbitals. This accounts for why the Fe 3d orbital character is absent in the top portion of the HO band. On going away from Γ, the HO band is strongly stabilized. At X (in the body-centered unit cell representation), unit cell orbitals must alternate their phases along the crystallographic a direction but keep a constant phase along the remaining two other crystallographic directions. This requirement can be met by combining

the π_4 and π_3 orbitals as shown in **10**, or by combining n_4 and

10

π_4 π_3
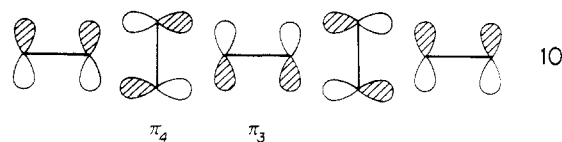
π_3 orbitals as shown in **11**. In both **10** and **11**, the interring P···P

11

π_3 n_4
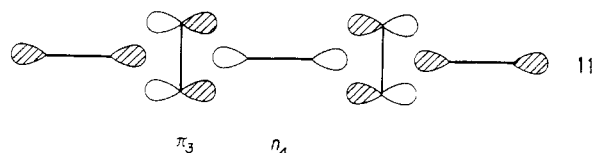
contacts have antibonding interactions as in **9**. However, π_3 and n_4 lie considerably lower in energy than π_4 (see Figure 3), so that the band orbitals **10** and **11** are lower in energy than **9**. This explains why the energy of the HO band is sharply lowered on going from Γ to X.

Our calculations show that the HOMO of the P_4^{4-} ring is antibonding in each P–P bond. The oxidation state of Ce (3+/4+) is higher than that of Eu (2+/3+) in RFe_4P_{12} (R = Ce, Eu). Thus, it is expected that the P–P bonds are longer in $CeFe_4P_{12}$ than in $EuFe_4P_{12}$, which is in agreement with experiment.[29]

Electrical Properties of Skutterudite Compounds

The Fermi surface of $LaFe_4P_{12}$ associated with the HO band is depicted in Figure 4, where the parallelepiped represents a prmitive reciprocal unit cell. For convenience, we show only one rounded octahedron-like Fermi surface at a corner of the parallelepiped in Figure 4, but such a sphere should be present at every corner of the parallelepiped. The rounded octahedron-like Fermi surface is consistent with the fact that the three crystallographic directions of $LaFe_4P_{12}$ are equivalent; i.e., $LaFe_4P_{12}$ is a three-dimensional metal. The Fermi level e_f occurs within the smallest DOS peak in Figure 2, so that the DOS value at e_f, $n(e_f)$, is not large, i.e., about (5 electrons/eV)/formula unit $LaFe_4P_{12}$. This value is close to the experimentally estimated one (($\sim$4 electrons/eV)/formula unit).[20] The $M_4X_{12}^{3-}$ lattices of $LaRu_4P_{12}$, $LaOs_4P_{12}$, $LaFe_4As_{12}$, $LaFe_4Sb_{12}$, $PrFe_4P_{12}$, and $NdFe_4P_{12}$ are isoelectronic with the $Fe_4X_{12}^{3-}$ lattice of $LaFe_4P_{12}$. Thus, all of them are expected to be metals, as observed experimentally.[9,13,21]

Part b of Figure 1 shows that the bottom of the e_g-block bands is separated from the top of the t_{2g}-block bands by a band gap of $\sim$2.7 eV. For the $Fe_4P_{12}^{4-}$ and its isoelectronic M_4X_{12} lattices, the t_{2g}-block bands of Figure 1 would be completely filled, so that the resulting electrical behavior should be semiconducting. This is consistent with the fact that the ternary skutterudites RFe_4P_{12} ($R^{4+} = Ce^{4+}$, U^{4+}) and $CeFe_4As_{12}$ and the binary skutterudites CoP_3, $RhAs_3$, $IrAs_3$, and $IrSb_3$ are semiconducting.[9,27]

Unlike $CeFe_4P_{12}$ and $CeFe_4As_{12}$, $CeFe_4Sb_{12}$ is a metal. Provided that the formal oxidation state of Ce is +4, the $Fe_4Sb_{12}^{4-}$ lattice would have its t_{2g}-block bands completely filled. Then the metallic properties of $CeFe_4Sb_{12}$ would imply that the top of its t_{2g}-block bands overlaps with the bottom of its e_g-block bands. To examine if this is possible, we perform band electronic structure calculations for the $Fe_4Sb_{12}^{4-}$ lattice. Parts a and b of Figure 5 summarize how the energies of the t_{2g}-block band top and the e_g-block band bottom vary as a function of the valence ionization potential H_{ii} (eV) and the exponent ζ of the Sb p orbital. It is quite obvious from Figure 5 that for any reasonable choice of these atomic parameters, the $Fe_4Sb_{12}^{4-}$ lattice always has a substantial band gap. Namely, the $Fe_4Sb_{12}^{4-}$ lattice cannot have the t_{2g}- and e_g-block bands overlap as in a semimetal. Therefore, the metallic character of $CeFe_4Sb_{12}$ cannot be explained if the oxidation state of Ce is +4 but can be explained when Ce is in the oxidation state of +3. Let us consider why the oxidation state of Ce is likely to

(29) Boonk, L.; Jeitschko, W.; Scholz, U. D.; Braun, D. J. *Z. Kristallogr.* **1987**, *178*, 30.
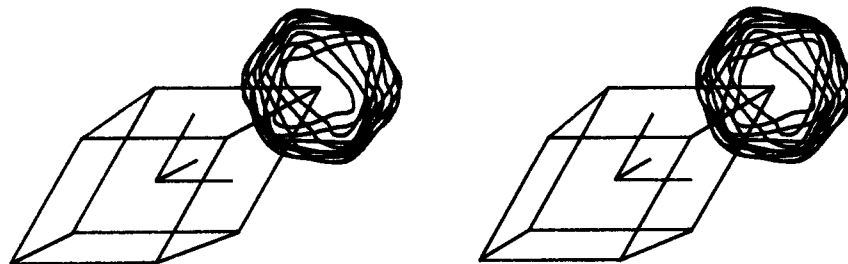
Figure 4. Stereodiagram of the Fermi surface associated with the HO band of Figure 1. Though not shown for simplicity, the rounded octahedron-like object should be present at each corner of the primitive unit cell.
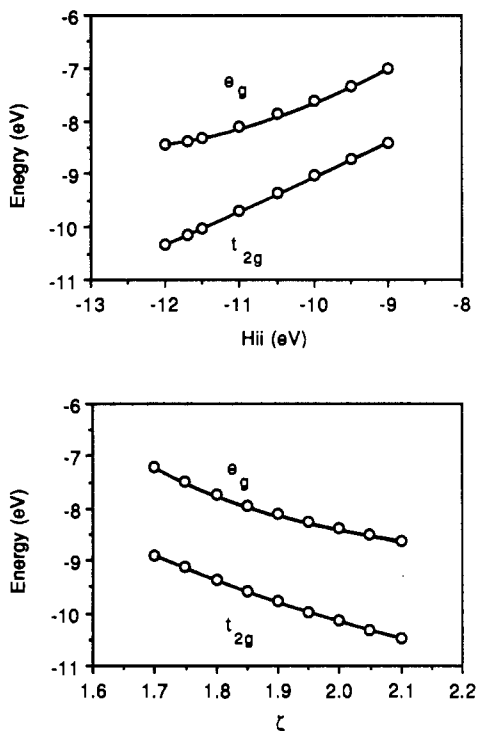
Figure 5. Band gap between the t_{2g}-block band top and the e_g-block band bottom of the Fe_4Sb_{12} lattice, calculated as a function of the valence shell ionization potential H_{ii} (with $\zeta = 1.999$) and the exponent ζ (with $H_{ii} = -11.7eV$) of the Sb 5p orbital.

be +3 for $CeFe_4Sb_{12}$. The HO band of the $Fe_4X_{12}^{4-}$ lattice is dominated by the π_4 orbital of the X_4^{4-} ring, so that the HO band for X = Sb lies higher in energy than that for X = P or As. Electron filling of the HO band would be energetically less favorable for X = Sb than for X = P or As. Therefore, it is likely that the Ce atoms of $CeFe_4Sb_{12}$ are in the +3 oxidation state.

Concluding Remarks

Our band electronic structure calculations on $LaFe_4P_{12}$ show that the HO band of the $Fe_4P_{12}^{3-}$ lattice has more phosphorus than Fe 3d orbital character in the vicinity of the Fermi level. Since electrons near the Fermi level are primarily responsible for superconductivity, this observation implies that the superconductivity of $LaFe_4P_{12}$ is primarily associated with the electrons of its phosphorus sublattice. According to Figure 2, the relative contribution of the Fe 3d orbitals increases when the Fermi level is lowered. To examine whether the superconductivity of $LaFe_4P_{12}$ originates largely from the iron or from the phosphorus atoms, it would be interesting to raise and lower the Fermi level of $LaFe_4P_{12}$ by doping La with Ce and Ba, respectively.

According to the present study, the two-electron bond model[8,9] for the skutterudites is essentially correct. Our calculations suggest that the M_4X_{12} lattice of any skutterudite structure would have its t_{2g}- and e_g-block bands separated by a band gap. Thus, an M_4X_{12} lattice with a formal d^6 electron count on the metal has completely filled t_{2g}-block bands and should be a semiconductor. Whether the binary skutterudites $CoAs_3$, $CoSb_3$, and RhP_3 are metallic or semiconducting has been controversial.[22-26] Since the M_4X_{12} lattices of these binary skutterudites are isoelectronic with the $Fe_4P_{12}^{4-}$ lattice of $LaFe_4P_{12}$, these three binary skutterudites should be semiconductors. According to this reasoning, a doped skutterudite phase $(Co_{1-x}Fe_x)P_3$, if made, is predicted to be a metal. The M_4P_{12} lattices of the binary NiP_3 and PdP_3[1,2] are isoelectronic with the $Fe_4P_{12}^{8-}$ lattice. Thus, within a rigid band approximation, the bottom portion of the e_g-block bands in part b of Figure 1 are partially filled, so that NiP_3 and PdP_3 are expected to be metallic.